Inoculating Stainless Steel with Titanium Nitride

W.J. Poole, A. Mitchell, and F. Weinberg

Department of Metals and Materials Engineering
University of British Columbia, Vancouver, B.C., Canada

Received June 2, 1997

ABSTRACT

The effectiveness of TiN as an inoculant for ferritic, austenitic, and ferrite/austenite stainless steel bars, solidified slowly and directionally, is examined. Without the addition of titanium and nitrogen to the steels, all solidified with a columnar structure. With sufficient additions of titanium and nitrogen the fully ferritic stainless steel (type 430) solidified with a well defined equiaxed structure. The steel with leading austenite dendrites (type 316 with 0.085 pct carbon) solidified with a columnar structure. The ferrite/austenite steels formed irregular equiaxed grains with poorly defined grain boundaries. The results are consistent with the lattice matching model for the inoculation of iron by TiN.

INTRODUCTION

Heterogeneous nucleation has been investigated extensively for a range of metals, primarily pure metals, with oxides, carbides and nitrides as nucleating agents. Bramfitt /1/ examined the effectiveness of carbides and nitrides as nucleating agents in the solidification of pure iron. He found that TiN was an effective nucleant, attributing this to good lattice fit on (100) planes of both the titanium atoms in the TiN and the iron atoms in the ferritic iron. On the basis of lattice matching, it follows that TiN would not be an effective inoculant for austenitic iron, since the lattice spacing of austenite (0.36773 nm) is appreciably larger than that of ferrite (0.29315 nm).

In addition to lattice matching the liquid would have to be supercooled for the TiN to nucleate grains. When steel solidifies under normal commercial conditions, there is no significant thermal supercooling in the bulk melt during solidification. For TiN inoculants to be effective under these conditions, supercooling must come from solute segregation, i.e. constitutional supercooling, where the local melt temperature is below the equilibrium liquidus temperature. An equiaxed grain can then form and grow at a TiN site in the supercooled melt surrounding it. There is no straightforward procedure for calculating the local solute segregation and constitutional supercooling which occurs in a commercial steel melt as it solidifies. In addition, solidification is dendritic, which makes the distribution of rejected solute at the interface complex.

An evaluation of the effectiveness of TiN as an inoculant is further complicated by the following factors. Stainless steels can solidify from the melt as ferrite, austenite, or both ferrite and austenite, depending on the composition of the steel, and the solidification conditions. After solidification the ferrite may transform to austenite on cooling, depending on the steel composition and the cooling rate. When transformations occur, the structure of the steel at the end of solidification cannot be directly determined from samples etched at room temperature. The combination of these factors makes evaluating the effectiveness of TiN as an inoculant uncertain.

The formation, distribution, and amount of ferrite and austenite in cast stainless steels have been examined as a function of melt composition and cooling rate /2-10/. It was shown that the percentage of ferrite in the casting at the end of solidification can be

estimated from the Cr_{eq}/Ni_{eq} ratio. Following Allan /10/, and Suutala and Moisio /6/

$$Cr_{eq} = \text{pct Cr} + 1.37(\text{pct Mo}) + 1.5(\text{pct Si}) + 2(\text{pct Nb}) + 3(\text{pct Ti})$$

$$Ni_{eq} = \text{pct Ni} + 22(\text{pct C}) + 14.2(\text{pct N}) + 0.31(\text{pct Mn}) + \text{pct Cu}$$

For Cr_{eq}/Ni_{eq} > 2, $Liq \rightarrow L + \delta \rightarrow \delta$

$= 1.5$ to 2.0, $Liq \rightarrow L + \delta \rightarrow L + \delta + \gamma \rightarrow \delta + \gamma$

$= 1.38$ to 1.5, $Liq \rightarrow L + \gamma \rightarrow L + \gamma + \delta \rightarrow \gamma + \delta$

< 1.38, $Liq \rightarrow L + \gamma \rightarrow \gamma$

where L is liquid, δ is the ferrite phase, and γ is the austenite phase.

At higher carbon contents, Hammar and Svensson /4/ reported that stainless steels solidify as austenite, with no ferrite present, when the carbon equivalent, C_{eq}, is greater than 0.065 wt pct, where C_{eq} = pct C + 0.65(pct N).

The process of formation of ferrite and austenite during solidification can be estimated from pseudo binary phase diagrams. These diagrams are constructed from the Fe/Cr/Ni ternary diagram with the iron concentration held constant. Phase diagrams for 70, 60, and 55 wt pct iron are shown by Brooks and Thompson /11/, who also point out that these diagrams are only approximations. Above about 75 wt pct iron with 15 wt pct chromium, the steel solidifies first as ferrite and then passes through a peritectic type reaction in which ferrite and liquid combine to form austenite. Between about 50 and 75 wt pct iron the steel passes through a eutectic type reaction in which both ferrite and austenite form from the melt. Following solidification, some ferrite may change to austenite by a solid state transformation.

The structure of austenitic stainless steels in welds has been examined extensively, as reviewed by Brooks and Thompson /11/. The weld structures are important, since the tendency for weld cracking is related to the weld structure. The present investigation considers solidification conditions typical of casting and directional solidification. In this cast growth velocities are in the range of 10×10^{-2} mm/s as compared to welding growth velocities /12/ of 10 mm/s. The large difference in growth velocities could result in markedly different solidification structures.

The effectiveness of TiN as an inoculant in stainless steel welds has been examined by a number of workers, as reviewed by Heintze /13/. It was observed that TiN is an effective inoculant in stainless steel welds when the steel solidifies entirely as ferrite, and is not effective when the steel solidifies entirely as austenite. Austenitic stainless steels which contain both ferrite and austenite may solidify with both phases forming during solidification. Heintze and McPherson /14/ reported that the structure of stainless steel welds, to which FeTi powder was added to the weld pool, consisted of columnar austenite with equiaxed retained ferrite along the core of the columnar grains. The columnar austenite resulted from the solid state transformation of the columnar ferrite which formed during solidification. Titanium alone is not effective, and only a fraction of the TiN particles present in the melt act as inoculants. The TiN particles are believed to be nucleated on aluminum or titanium oxide particles in the melt, based on the observation of oxide particles in the centre of the TiN particles.

In the present investigation the effectiveness of TiN as an inoculant is determined experimentally, for ferritic and austenitic stainless steels solidified unidirectionally at slow growth rates. The inoculant is generated in the melt by the reaction of ferrotitanium and high nitrogen ferrochromium, at levels which are considerably greater than the reported saturation solubility of TiN in these alloys.

PROCEDURE

The apparatus for melting and solidifying the steel is shown in Figure 1. The concentrations of the alloying elements and residuals in the steels examined, as determined by emission spectroscopy, are listed in Table 1. The test sample consists of a steel bar 25 mm in diameter and 300 mm in length with a hole along the axis of the bar 6.3 mm in diameter. The steel bar is contained in a close fitting ceramic tube which is contained in a larger diameter quartz tube, as shown in the figure. Two Pt/Pt10%Rh thermocouples, in ceramic closed end sheaths, are inserted into the bar along the central hole, one from each end of the bar. One thermo-

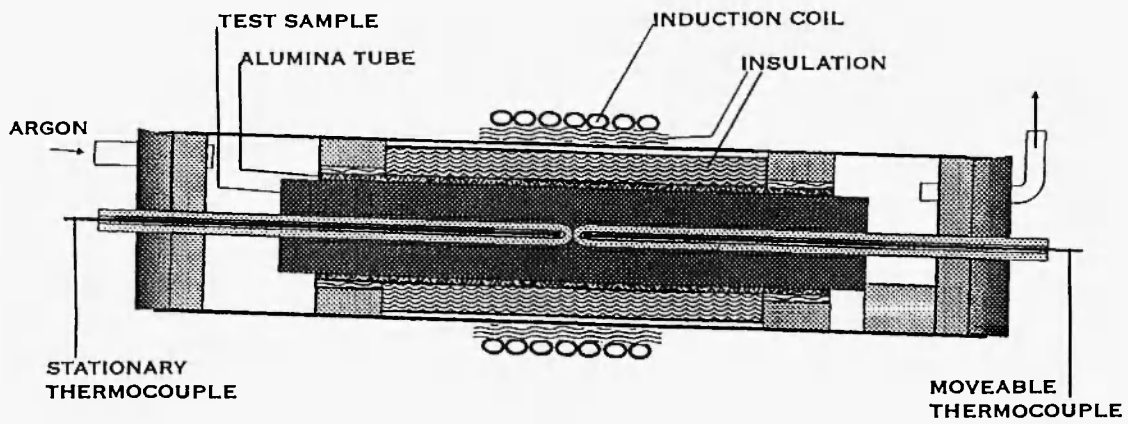

Fig. 1: Apparatus for melting and solidifying stainless steel bars.

Table 1
Stainless Steel Compositions – wt pct

Test No	Steel	Added	C	Ti	N	Cr	Ni	Mo	Mn	Si	Cu
9	430		0.10			18.5	0.27	0.10	0.47	0.44	0.05
10	316		0.015			16.6	10.1	2.20	1.40	0.47	0.20
11	430	Ti+N	0.080	0.62	0.010	18.5	0.27	0.10	0.47	0.48	0.05
12	304	Ti+N	0.054	0.72	0.010	19.5	8.0	0.17	1.90	0.45	0.21
13	316	Ti+N	0.020	0.69	0.015	16.2	10.6	2.30	1.27	0.42	0.28
14	316	Ti+N	0.020	0.44	0.017	16.9	10.0	2.22	1.42	0.51	0.28
15	316	C	0.085			17.1	10.4	2.00	1.35	0.60	0.19
16	316	Ti+N+C	0.085	0.56	(0.013)	17.0	10.1	2.00	1.30	0.60	0.17
17	316	Ti+N+C	0.080	0.74	(0.014)	16.2	10.1	2.00	1.20	0.60	

S and P less than 0.03 wt pct; Al less than 0.6 wt pct

couple is positioned in the middle of the bar. The other thermocouple is moved along the axis of the bar during the test, inside the ceramic sheath. Thermal data from the second thermocouple enables the growth velocities and temperature gradients during solidification to be established. The quartz tube is tilted 5° from the horizontal in order to keep the cavities, resulting from solidification, in the upper half of the test bar. Temperature measurements along the axis are made in the lower half of the bar. In a test, the middle section of the bar is slowly heated by the induction coil at a frequency of 10 kHz, held for a short period, and then slowly cooled by gradually reducing the power to the coil. Approximately 23 cm of the bar is melted, with 3.5 cm solid at either end. The freezing rate is controlled by the rate at which the power to the coil is reduced.

Samples are inoculated with FeTi containing 70 wt pct titanium, and Cr[Fe]N containing 6.63 wt pct nitrogen. Small pieces of the inoculating material, which dissolve in the melt, are placed in a slot 6 mm square and 150 mm long, machined along the top surface of the centre of the bar. The amount added to the melt and the amount recovered in the steel are listed in Table 2. In Tests 15-17 a high level of carbon was required in the steel. To obtain this, charge ferrochromium with high carbon was added to the melt, as well as the titanium and nitrogen.

To determine the interior cast structure of the

samples a flat surface was ground along the length of the steel bar producing a surface approximately 17 mm wide. The ground surface was then etched in a 1:1:1 solution of $HCl/HNO_3/H_2O$, or a ferric chloride etchant given by Villafuerte and Kerr /15/, to delineate the grain structure. Samples were then cut from the equiaxed region of the bar. Some samples were polished and examined in the SEM to observe the TiN inclusions in the steel, others polished and etched to delineate the cast structure more clearly, and others used for compositional analysis. To delineate the cast microstructure, a colour etching reagent given by Allan was used /10/, as well as an etchant consisting of 10 ml HNO_3, 10 ml acetic acid, 15 ml HCl, and two to three drops of glycerine.

OBSERVATIONS

1. Ferritic Stainless Steels

When titanium and nitrogen were added to the type 430 ferritic stainless steel (Test 11), the columnar grains were replaced by small, well defined, equiaxed grains of approximately 1.3 mm in diameter, as shown in Fig. 2(A) and listed in Table 2. The Cr_{eq}/Ni_{eq} for this steel is 7.23 (Table 3), which is higher than the critical ratio of 2.0, referred to previously, above which the structure is entirely ferritic. The change from columnar to equiaxed grains in the ferritic steel, with the addition of TiN, is consistent with the lattice matching model.

2. Ferritic/Austenitic Stainless Steels

For the type 304 and 316 stainless steels, adding titanium and nitrogen also resulted in the columnar grains being replaced by small grains of about 0.5 mm in diameter. The etched surfaces of these steels, using the ferric chloride etchant, are shown in Figures 2(b) and 2(c) respectively. Both structures are similar, exhibiting a highly irregular structure with poorly defined grain boundaries. Similar observations are

Table 2
Casting and Inoculation Data

		Columnar Zone			Inoculant Added					
Test No	Steel	L mm	V_c mm/s $x10^{-2}$	W mm	Ti wt pct added	Ti wt pct comp	N wt pct added	N wt pct comp	V_e mm/s $x10^{-2}$	D mm
9	430	73	7	2	0		0			
10	316	80	33	4	0		0			
11	430				1	0.62	0.05	0.010	11	1.3
12	304				1	0.72	0.05	0.010	13	0.5
13	316				1	0.69	0.05	0.015	8.0	0.4
14	316				0.5	0.44	0.025	0.017	7.7	elong
15	316	75	14	2-6	0	0.0	0			
16	316	80	17	2-6	1	0.56	0.05			
17	316	97	11	4-7	1	0.74	0.05			

L = length of the columnar zone on each side of the bar

V_c, V_e = freezing rate in the columnar and equiaxed zone

W = width of the columnar grains

D = diameter of the equiaxed grains

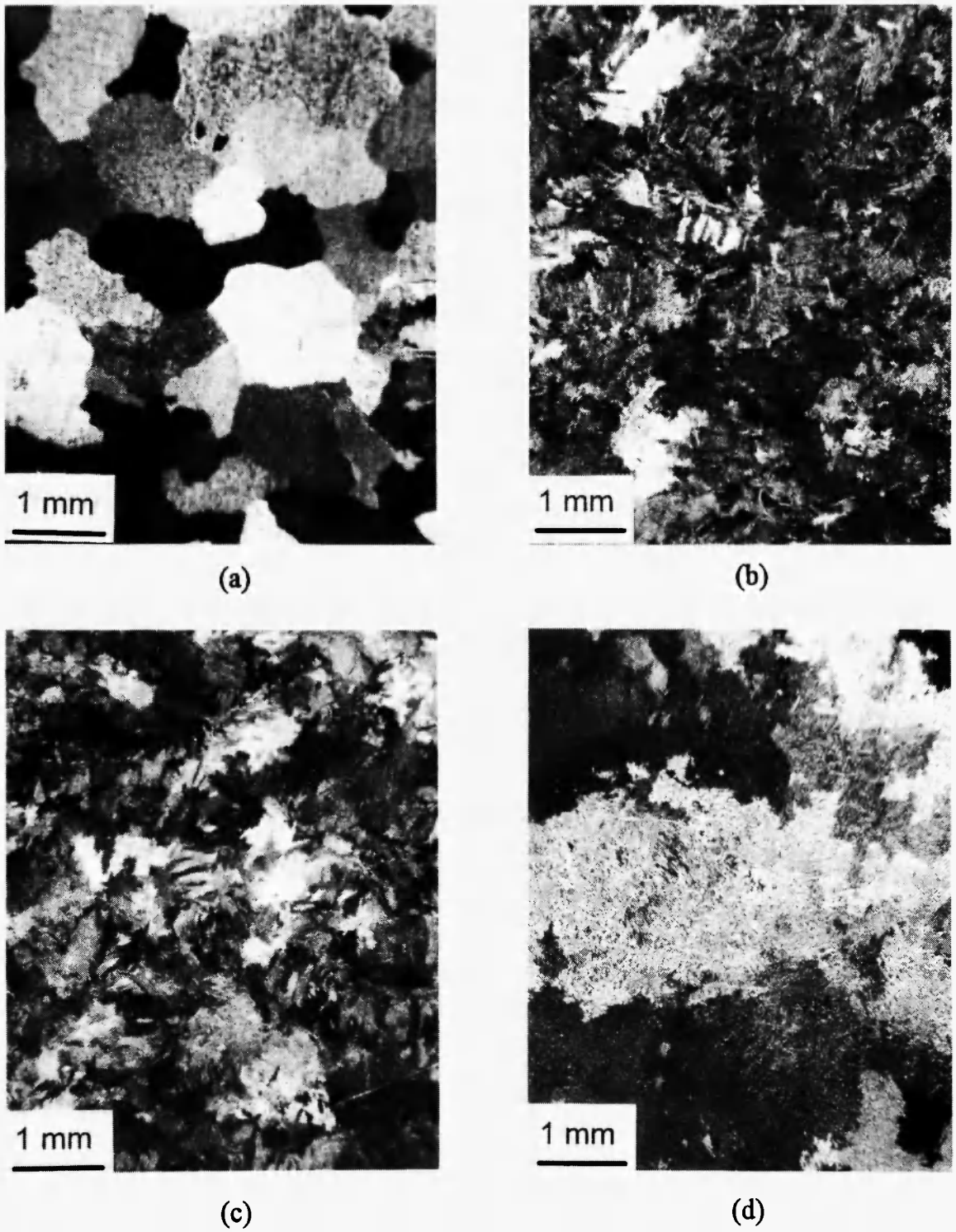

Fig. 2: Grain structure in stainless steel bars inoculated with TiN: (a) 430 (Test 11), (b) 304 (Test 12), (c) 316 (Test 13), (d) Inoculated with less Ti: 316 (Test 14).

Table 3
Chromium and Nickel Equivalents

Test	Steel	Cr_{eq}	Ni_{eq}	Cr_{eq}/Ni_{eq}
9	430	19.30	2.67	7.23
10	316	20.32	11.06	1.83
11	430	21.22	2.23	9.52
12	304	22.57	10.00	2.26
13	316	22.05	11.71	1.88
14	316	22.03	11.16	1.97
15	316	20.74	12.88	1.61
16	316	22.32	12.54	1,78
17	316	22.06	12.49	1.77

reported for austenitic stainless steels by Suutala *et al.* /16/. The Cr_{eq}/Ni_{eq} for type 304 steel is 2.26 indicating the steel should be entirely ferritic. For the type 316 steel Cr_{eq}/Ni_{eq} is 1.88 indicating ferrite should form first during solidification, followed by austenite. Therefore, on the basis of the Cr_{eq}/Ni_{eq} ratio, the type 304 steel should have the same structure as type 430, and type 316 should be different. This is not what was observed.

Etching the steel samples in the colour etchant of Allan /10/ indicated that the samples consisted primarily of austenite, with small irregular regions of residual ferrite. Etching the samples in the microetchant reagent produced the structure shown in Figure 3. The structure consists of small light regions surrounded by dark bands, similar to the structures shown by Brooks and Thompson /11/ for welded stainless steels. They describe the light regions as austenite and the dark bands as residual ferrite.

As a further test of the effectiveness of TiN as an inoculant, the amount of titanium and nitrogen added to the melt was reduced by a factor of two. The resultant structure for type 316 stainless steel (Test 14) consisted of both elongated, large equiaxed grains, and irregular columnar grains, as shown in Figure 2(d). The appearance of the structure on a microetched sample at higher magnification is shown in Figure 4, consisting of irregular rod segments in a continuous matrix. To determine whether the rod segments on the etched surface were austenite and the material between

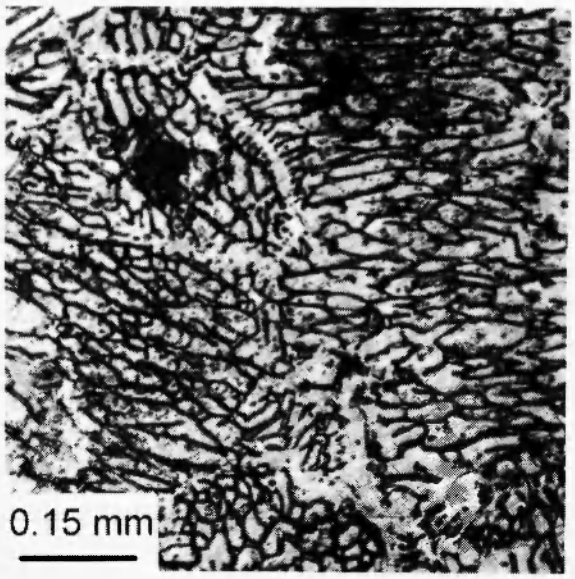

Fig. 3: Etched surface of type 304 stainless steel (Test 12) showing light areas (austenite) separated by dark bands (ferrite).

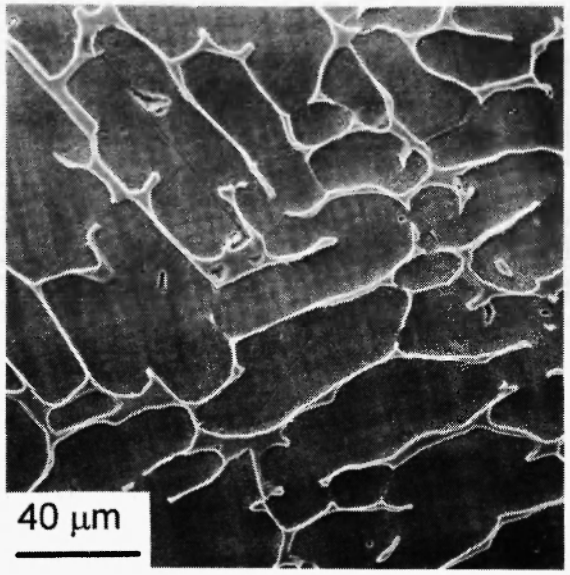

Fig. 4: Etched surface of type 316 stainless steel showing irregular ferrite rods in an austenite matrix.

the rods ferrite, the concentration of chromium and nickel in both regions was measured using EDX. From Hammar and Svensson /4/, for adjacent regions of ferrite and austenite, the ratio of the chromium concen-

tration in the ferrite over that in the austenite is 1.40, and of nickel 0.60. Four sets of measurements of adjacent rods and matrix were made in an area similar to that shown in Figure 4 and in all cases the chromium ratio between the rods and matrix was 1.4 and the nickel ratio 0.5. This clearly indicates that the rods are ferrite and the matrix austenite. The large columnar and equiaxed grain structures observed, with a decrease in the levels of added titanium and nitrogen, are consistent with a marked reduction in the number of effective TiN nucleating particles in the melt during solidification.

3. Austenitic Stainless Steel

To examine the effect of TiN in fully austenitic stainless steels, a 316 type stainless steel with additions of carbon was tested. Hammar and Svensson /4/ reported that this steel solidifies entirely as austenite with carbon levels above 0.065 wt pct. In the present experiments the carbon level of the steel was raised to 0.085 wt pct which is well above the specified level. The Cr_{eq}/Ni_{eq} for the steels with carbon, titanium and nitrogen added (Tests 16, 17) is 1.78. This value of the ratio indicates that ferrite should solidify first, followed by austenite, which is contrary to the results reported by Hammar and Svennson /4/, where only austenite solidifies. Without the titanium and nitrogen additions (Test 15) the length of the columnar region was 75 mm, similar to that of the corresponding steel without the carbon addition (Test 10). With titanium and nitrogen additions (Tests 16 and 17), the columnar structure was maintained, with no equiaxed grains evident for growth velocities of 17 and 11 x 10^{-2} mm/s. If the structure was fully austenitic, following Hammar and Svennson /4/, the results show that TiN is not an effective nucleant in fully austenitic stainless steels, consistent with the lattice matching model.

Examples of the cast structure of samples from Tests 15, 16 and 17, after etching in the colour etch, showed that the steels were not entirely austenitic. The structure consisted of long austenite dendrites, rich in nickel, with small irregular islands of ferrite or chromium rich austenite within the dendrite branches. Narrow irregular ferrite strips were also observed in the interdendritic regions along with higher chromium concentrations. Measurements of the ratio of chromium concentration in the interdendritic ferrite divided by the chromium concentration in the dendrite arm gave a ratio close to 1.4, which confirmed that the interdendritic phase was ferrite. The ferrite observed in the interdendritic regions would form towards the end of solidification and thus would not result in equiaxed grains if nucleation of ferrite on TiN particles occurred. The small ferrite regions within the dendrite branches are likely due to solid state phase transformations associated with solute segregation during solidification. Small ferrite islands within austenite dendrite arms have been observed by Fredriksson as reported by Brooks and Thompson /11/.

4. TiN Particles

To establish that TiN particles were present in the steels to which titanium and nitrogen were added, polished sections of the equiaxed region of Tests 11 and 12 were examined for particles with an SEM. Large faceted yellow block particles were observed, as well as irregular elongated dark inclusions. An example of the yellow block particles, in a clump, is shown in Figure 5(a). Analysis by EDX showed the particles to be rich in titanium, which is illustrated by the titanium dot map of the same area shown in Figure 5(b). The particles were also shown to be rich in nitrogen using WDX. The titanium and nitrogen peaks in the analysis overlap, but the centres of the peaks are sufficiently separated to establish clearly the presence of a strong nitrogen peak. All of the particles shown in Figure 5(a) were contained in one grain. In several areas on a polished surface, particles were observed with a density of about 9 x $10^2/mm^2$ which were contained in several grains. These observations indicate that only a fraction of the TiN particles in the melt acted as nucleating sites in agreement with Heintze and McPherson /16/. The dark elongated inclusions were also observed to be rich in titanium and parts of the inclusions rich in nitrogen. The titanium and nitrogen in the inclusions may be a result of the segregation of these elements, during solidification, to the interdendritic regions. If this has occurred, any TiN particles incorporated in these inclusions would not be effective nucleating sites.

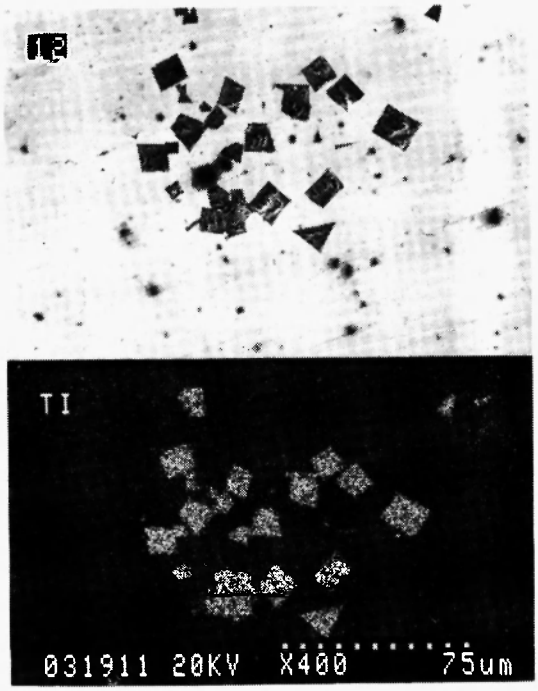

Fig. 5: TiN inclusions: Top: A faceted clump of TiN inclusions from Test 12. Bottom: Corresponding titanium map showing inclusions are titanium rich.

DISCUSSION

The present results for ferritic type 430 stainless steel (Test 11) are in agreement with the inoculation theory. This steel solidifies entirely as ferrite, consistent with a Cr_{eq}/Ni_{eq} ratio of 7.23 which is well above the value of 2.0 given by Suutala /6/ for the onset of ferritic growth. TiN particles form in the melt, prior to the onset of solidification, following Ozturk *et al.* /17/ as discussed below. The solidification structure consists of columnar grains grown at slow solidification rates without TiN present, and well defined equiaxed grains for the same growth rates with TiN present. The basis of the inoculation theory is that there is good lattice matching on (100) planes between the titanium atoms in the TiN and the iron atoms in the ferritic iron. The theory is based on experiments with pure iron. From the present results it is demonstrated that the theory also applies to ferritic stainless steels with solute and residual atoms present, solidified at slow growth rates.

As the melt cools, the titanium and nitrogen in solution form TiN particles prior to the onset of solidification. The thermochemistry of the formation of the TiN particles in stainless steel melts has been examined by Ozturk *et al.* /17/ who derived the temperature dependence of the saturation solubility of TiN in the alloys as a function of composition. As an example of their results, they show that solid particles of TiN form in the melt in stainless steel containing 18 wt pct Cr, 8 wt pct Ni, 0.5 wt pct Ti and 0.0118 wt pct N which is cooled from 1600°C. Particle growth is completed by 1500°C. As the TiN forms, the titanium concentration in the melt drops a small amount, from 0.50 to 0.47 wt pct, and the nitrogen an appreciable amount, from 0.0118 wt pct to 0.0038 pct. The steel compositions in this investigation are similar to those examined by Ozturk *et al.* /17/. Accordingly, in calculating the Cr_{eq} and Ni_{eq} it may be assumed that the formation of TiN has little effect on the titanium concentration in the melt, and effectively takes up all the nitrogen in the melt. It has been proposed /14,15/ that TiN particles nucleate on Al_2O_3 particles in the melt. This was not examined in this investigation.

The TiN particles which form in the melt may be uniformly distributed in the melt or be clumped. If the particles form clumps, this could result in a wide range of grain sizes, smaller grains being associated with the clumped TiN particles. Kivineva *et al.* /18/ reported that some particles added to the weld pool in stainless steel welds exhibited clumping. Titanium carbide particles were observed to be concentrated between dendrite arms, from which they concluded that particles were pushed into the interdendritic region by the advancing solid/liquid interface.

Particle pushing by an advancing solid/liquid interface was examined by Schvezov and Weinberg /19/ for iron particles between 3 and 30 μm in diameter in molten lead. They found no evidence of particle pushing by a plane solid/liquid interface. For cellular and dendritic interfaces, some particles were concentrated in the cell walls and between dendrite arms which was attributed to fluid flow and buoyancy forces, not particle pushing. Clumping of particles may be associated with a tendency for solid materials in a liquid to stick when the density of the solids is close to

that of the liquid, as reported by Weinberg and Schvezov /20/.

The austenitic type 304 and 316 stainless steels containing TiN were observed to have small grained equiaxed structures with poorly defined grain boundaries. The Cr_{eq}/Ni_{eq} ratio of the 304 steel was 2.26 and of the 316 steel 1.88 which should result in the former solidifying entirely as ferrite and the latter as ferrite followed by austenite. As pointed out by Brooks and Thompson /11/, the Cr_{eq}/Ni_{eq} ratios should be considered as only general indicators of the cast structure. It then appears that the Cr_{eq}/Ni_{eq} ratios of the 304 and 316 steels are sufficiently close together to solidify with similar structures.

In both steels ferrite dendrites form at the start of solidification. These dendrites nucleate readily on TiN particles in the melt beginning an equiaxed structure. The observation of an irregular grain structure may result from two processes.

(a) As the dendrites grow and nickel segregates into the melt, a peritectic reaction may occur in which the ferrite and liquid react to form austenite. Austenite does not readily nucleate on ferrite since, as with TiN, the lattice spacing of austenite is large compared to that of ferrite. In addition, for the ferrite/liquid reaction to proceed, diffusion of solute through the austenite is required, which is slow. As a result of both effects the growth process will slow down and the remaining liquid can then become appreciably supercooled. This may result in the nucleation and growth of austenite in the interdendritic liquid on the ferrite, or the nucleation of very small austenite grains in the liquid. Large supercooling will also result in the growth of fine dendrites, resulting in a highly irregular interphase morphology and poorly defined grain boundary.

(b) Irregular grain boundaries may also be a result of the solid state transformation of ferrite to austenite in which a lathy ferrite structure is produced, as described by Brooks and Thompson /11/. The phase transformation may cause a change in the morphology of the prior ferrite grains.

The present results do not clearly indicate whether a peritectic reaction has occurred during solidification. It is also not clear which regions solidified as ferrite and transformed to austenite on cooling, and which solidified as austenite. It is possible that austenite solidified in the regions where the observed chromium and nickel concentrations in the rod cells and the cell walls were nearly the same. Ferrite would then have solidified in the regions in which the observed chromium concentration was appreciably higher in the cell walls.

Reducing the titanium and nitrogen additions by a factor of two changes the solidification structure from small grains to a mixture of columnar, elongated, and small grains. From the stability diagram for TiN given by Ozturk *et al.* /17/, TiN particles will form at the lower concentration levels as the melt cools. The change in structure is then associated with a reduction in the number of nucleating TiN particles in the melt.

CONCLUSIONS

1. TiN is an effective inoculant for ferritic stainless steels which have been solidified slowly and directionally. This is the case for type 430 stainless steel which solidifies as ferrite. Without titanium and nitrogen additions in the melt, the solidification structure is columnar. Adding 1 wt pct titanium and 0.05 wt pct nitrogen results in a well defined equiaxed structure.
2. With steels which solidify primarily as austenite, TiN is not an effective inoculant. For a type 316 stainless steel containing 0.085 wt pct carbon, solidification occurs primarily by the growth of austenite dendrites. For this steel, adding titanium and nitrogen to the melt has no effect on the columnar structure formed during solidification.
3. Ferrite/austenite stainless steels, in which ferrite is the leading phase during solidification, are inoculated by TiN. For types 304 and 316 stainless steels inoculation was effective when 1 wt pct titanium and 0.05 wt pct nitrogen was added to the steel. The solidified structure of small grains was highly irregular with poorly defined grain boundaries. TiN was not effective when 0.5 wt pct titanium and 0.025 wt pct nitrogen were added to the steel.
4. The present results of the inoculation of stainless steels by TiN are consistent with the lattice matching model for the inoculation of iron by TiN given by Bramfitt /1/.

ACKNOWLEDGEMENTS

The work was supported by NSERC. We wish to thank Mark Wolters and Dionne Mackinnon for assistance with the experimental work.

REFERENCES

1. B.L. Bramfitt, *Met. Trans.*, **1**, 1987-1995 (1970).
2. A.L. Schaeffler, *Welding Journal*, **20**, 601s-620s (1947).
3. H. Fredriksson, *Met. Trans.*, **3**, 2989-2997 (1972).
4. O. Hammar and U. Svensson, *Solidification and Casting of Metals*, The Metals Society, 1977; 401-410.
5. M. Bobadilla and G. Lesoult, *Solidification and Casting in the Foundry and Casthouse*, The Metals Society, 1980; 304-309.
6. M. Suutala and T. Moisio, *Solidification and Casting in the Foundry and Casthouse*, The Metals Society, 1980; 310-314.
7. M.T. Leger, *Stainless Steel Castings*, ASTM Publication 04-756000-01, 1982; 105-125.
8. L.S. Aubrey, P.F. Wieser, W.J. Pollard and E.A. Schoefer, *Stainless Steel Castings*, ASTM Publication 04-756000-01, 1982; 126-164.
9. JERNKONTORET, *A Guide to the Solidification of Steels*, Stockholm, Sweden, 1977.
10. G.E. Allan, *Ironmaking and Steelmaking*, **22**, 465-477 (1995).
11. J.A. Brooks and A.W. Thompson, *Int. Mat. Rev.*, **36**, 16-44 (1991).
12. J.C. Villafuerte, E. Pardo and H.W. Kerr, *Met. Trans. A*, **21A**, 2009-21019 (1990).
13. G.N. Heintze, *Australian Welding Research*, 32-44 (1984).
14. G.N. Heintze and R. McPherson, *Australian Welding Journal*, 37-40 (1983).
15. J.C. Villafuerte and H.W. Kerr, *Met. Trans. A*, **21A**, 979-986 (1990).
16. N. Suutala, T. Takalo and T. Moisio, *Met. Trans. A*, **11A**, 717-725 (1980).
17. B. Ozturk, R. Mataway and R.J. Fruehan, *Met. Trans. B*, **26B**, 563-567 (1995).
18. E.I. Kivineva, D.L. Olson and D.K. Matlock, *Welding Journal*, 74, 83s (1995).
19. C.E. Schvezov and F. Weinberg, *Met. Trans. B*, **16B**, 367-375 (1985).
20. F. Weinberg and C.E. Schvezov, *Met. Trans. B*, **25B**, 397-403 (1994).